Macromolecules
ARTICLE

Macromolecules **2010**, *43*, 845–855 **845**
DOI: 10.1021/ma902119p

Pseudoperiodic "Living" and/or Controlled Cationic Ring-Opening Copolymerization of Oxetane with Tetrahydropyran: Microstructure of Polymers vs Kinetics of Chain Growth

Hassen Bouchékif,*,‡,† Marcia I. Philbin,§ Eamon Colclough,§ and Allan J. Amass*,‡

†*Department of Chemistry, Biomolecular Sciences Program, Laurentian University, 935 Ramsey Lake Rd, Sudbury, Ontario PE 2C6, Canada,* ‡*Aston University, School of Chemical Engineering & Applied Chemistry (CEAC), Birmingham B4 7ET, United Kingdom, and* §*QinetiQ (DERA) Fort Halstead, Sevenoaks, Kent TN14 7BP, United Kingdom*

Received September 24, 2009; Revised Manuscript Received December 4, 2009

ABSTRACT: The "living" and/or controlled cationic ring-opening bulk copolymerization of oxetane (Ox) with tetrahydropyran (THP) (cyclic ether with no homopolymerizability) at 35 °C was examined using ethoxymethyl-1-oxoniacyclohexane hexafluoroantimonate (EMOA) and $(BF_3 \cdot CH_3OH)_{THP}$ as fast and slow initiator, respectively, yielding living and nonliving polymers with pseudoperiodic sequences (i.e., each pentamethylene oxide fragment inserted into the polymer is flanked by two trimethylene oxide fragments). Good control over number-average molecular weight (M_n up to 150 000 g mol^{-1}) with molecular weight distribution (MWD $\sim$ 1.4−1.5) broader than predicted by the Poison distribution (MWDs $> 1+1/DP_n$) was attained using EMOA as initiating system, i.e., $C_2H_5OCH_2Cl$ with 1.1 equiv of $AgSbF_6$ as a stable catalyst and 1.1 equiv of 2,6-di-*tert*-butylpyridine used as a non-nucleophilic proton trap. With $(BF_3 \cdot CH_3OH)_{THP}$, a drift of the linear dependence $M_{n(GPC)}$ vs $M_{n(theory)}$ to lower molecular weight was observed together with the production of cyclic oligomers, ~3−5% of the Ox consumed in THP against ~30% in dichloromethane. Structural and kinetics studies highlighted a mechanism of chains growth where the rate of mutual conversion between "strain ACE species" (chain terminated by a tertiary 1-oxoniacyclobutane ion, A1) and "strain-free ACE species" (chain terminated by a tertiary 1-oxoniacyclohexane ion, T1) depends on the rate at which Ox converts the stable species T1 (kind of "dormant" species) into a living "propagating" center A1 (i.e., k_a^{app}[Ox]). The role of the THP solvent associated with the suspension of irreversible and reversible transfer reactions to polymer, when the polymerization is initiated with EMOA, was predicted by our kinetic considerations. The activation−deactivation pseudoequilibrium coefficient (Q_t) was then calculated in a pure theoretical basis. From the measured apparent rate constant of Ox (k_{Ox}^{app}) and THP ($k_{THP}^{app} = k_{a(endo)}^{app}$) consumption, Q_t and reactivity ratio (k_p/k_d, $k_{a(endo)}/k_{a(exo)}$, and $k_s/k_{a(endo)}$) were calculated, which then allow the determination of the transition rate constant of elementary step reactions that governs the increase of M_n with conversion.

Introduction

The cationic ring-opening polymerization of cyclic ethers via active chain end (ACE) mechanism has received considerable attention since the 1950s.[1] The mechanism kinetics have been established for many systems, based on the concentration of the propagating species (tertiary oxonium ions), which were determined either by phenoxy end-capping[2−5] or by proton,[6−10] carbon,[11] and/or fluorine[12−18] NMR spectroscopy. In the polymerization of oxolane (THF)[19,20] and oxepane (OXP),[21] e.g., initiated by 1,3-dioxolan-2-ylium salts (a very rapid and quantitative initiator), a true equilibrium polymerization[22] was proposed, without apparent chain-ends annihilation, producing a straight "living" polyether. In those systems, reversible transfer (i.e., depropagation) contributes to the fall off M_n's to the equilibrium value and subsequently a widening of molecular weight distribution, which is initially Poison type and eventually reaches a broad exponential/Flory−Schulz "most probable" distribution at the equilibration.[7,8] If polymer with predictable M_n and narrow molecular weight distribution (M_w/M_n) are required, polymerization in those systems must be limited to low conversion. The main characteristic of equilibrium polymerization is also found in the living polymerization of THF[9,10] and OXP[18] initiated with superacid esters, though reversible termination (i.e., macroions ↔ macroester equilibrium) has only a slight influence on the molecular weight distribution of the polymer formed under equilibrium conditions.[7,8,22] The three-[6,23−28] and four-membered[5,7,8,12,13,29−37] cyclic ethers monomers are highly strained rings, and thus no polymerization equilibrium can be expected (i.e., polymerization are almost quantitative); only the macroester can be observed in reversible termination,[6,12,13] and inter- and intramolecular transfer reactions occur more significantly.

Recently, we reported a new synthetic route that allows "living" and/or controlled cationic ring-opening polymerization oxetane (Ox) in 1,4-dioxane (1,4-D) (cyclic ether which has no homopolymerizability) solvent.[38,39] In this system (Scheme 1c), the solvent is used to end-cap the strain tertiary 1-oxoniacyclobutane ions A1 (rate constant k_d), producing a less reactive terminal tertiary 1-oxonia-4-oxacyclohexane group T1. As T1 is less reactive, then there is greater discrimination between the more nucleophilic oxygen atom in Ox (rate constants $k_{a(exo)}$ and $k_{a(endo)}$) and in 1,4-D (rate constant k_s) than the less nucleophilic polymer chain ether oxygen atoms (see Figure 1),[42,46] suspending reversible transfer, backbiting, and intermolecular transfer reactions as it occurs in normal polymerization of Ox in non-nucleophilic

*To whom correspondence should be addressed. E-mail: hbouchekif@yahoo.fr (H.B.); a.j.amass@aston.ac.uk (A.J.A.).

Published on Web 12/30/2009

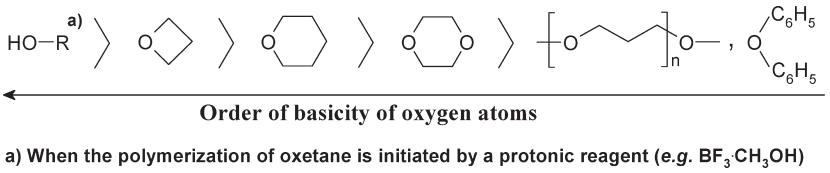

Figure 1. Order of basicity of oxygen atoms[41−44] present during the cationic ring-opening polymerization of oxetane.

Scheme 1. Mechanism Proposed in Cationic Ring-Opening Polymerization of Oxetane via Active Chain End (ACE) Mechanism in Dichloromethane (DCM), in 1,4-Dioxane (1,4-D), and in Tetrahydropyran (THP) at 35 °C

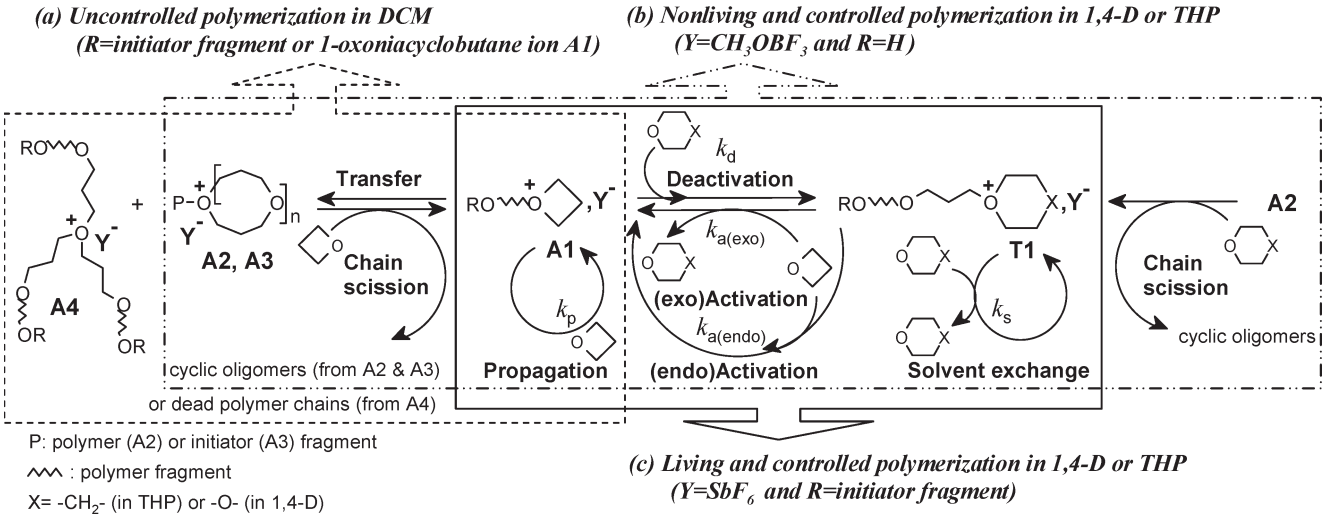

dipolar aprotic solvent (Scheme 1a).[5,7,8,12,13,29−37] Using phenoxypropyl-1-oxonia-4-oxacylohexane hexafluoroantimonate (structure equivalent to T1) as initiator yielding fast and instant initiation (i.e., $k_i \geq k_{a(exo)} > k_{a(endo)}$), poly(oxetane-*co*-1,4-dioxane) (which possess 2% of 1,4-D fragment) with predictable number-average molecular weight (up to 160 000 g mol^{-1}) and narrow PDI (~1.2−1.3) was produced successfully.[38,39] The use in 1,4-D of initiator (e.g., $(BF_3{\cdot}CH_3OH)_{1,4\text{-}D}$) yielding growing α-(hydroxyl)polyoxetane oxonium ions (Scheme 1b) was found to not be beneficial for the control of the polymerization as a subsystem[39] of cyclic oligomers formation can also proceed from those growing chains failing to reach the sufficient length to entropically[40,41] disfavor the end-to-end ring closure reaction. Further investigations in dichloromethane (DCM) showed that cyclic oligomers formation by initiated end-biting reaction can be enhanced against chain growth by using diphenyl ether (i.e., less nucleophilic than polymer chain ether oxygen atoms) as end-capping agent.

Because the oxygen atom in tetrahydropyran (THP) (cyclic ethers that do not homopolymerize[11]) is more nucleophilic than the oxygen atoms of 1,4-D[42−46] but also less nucleophilic than the oxygen atom of the oxetane molecule, the cationic ring-opening polymerization of Ox in THP solvent was then examined using ethoxymethyl-1-oxaniacylohexane hexafluoroantimonate (EMOA) (structure equivalent to T1) and $(BF_3{:}CH_3OH)_{THP}$ as initiator, yielding respectively living and nonliving polymers. In this article, we report the preparation of an amorphous copolymer (i.e., poly((oxetane)$_x$-*co*-(tetrahydropyran)$_{1-x}$) with $x < 0.3$) with pseudoperiodic sequences (i.e., each pentamethylene oxide fragment inserted into the polymer is flanked by two trimethylene oxide fragments)), well-controlled DP_n (= $\Delta([Ox] + [THP])/[initiator]_0$), and MWDs broader than predicted by Poison distribution (MWDs > $1 + 1/DP_n$). Our results on copolymer microstructures obtained at the triad level will be discussed and use to evaluate and to test the model developed to describe the bulk copolymerization of Ox with THP. For this purpose, an experimental design was envisaged in which the copolymerization of Ox with THP exhibit a "living" and controlled character. This is illustrated in the Figure 3 when the bulk copolymerization of Ox with THP is initiated by EMOA at 35 °C. In this study, the activation−deactivation pseudoequilibrium coefficient (Q_t) describing the process of "equilibration" (i.e., T1 + THP → k_sT1 + THP) and mutual conversion between A1 and T1 was calculated in a pure theoretical basis. From the measured apparent rate constant of Ox (k_{Ox}^{app}) and THP ($k_{a(endo)}^{app}$) consumption, Q_t and reactivity ratio (k_p/k_d, $k_{a(endo)}/k_{a(exo)}$, and $k_s/k_{a(endo)}$) can then be calculated, which then allows the determination of the transition rate constant of elementary step reactions involved in the process of chains growth (Scheme 2).

Experimental Section

Materials. Oxetane (Alfa Aesar, 99%), tetrahydropyran (Aldrich, ≥98.0%), and dichloromethane (DCM) Hi-dry (Romil Pure Chemistry Co., >99.9%) were dried over calcium hydride for 48 h and distilled before use. Ox and THP were further purified by refluxing over sodium/benzophenone radical anion and then distilled before use. Boron trifluoride−methanol complex (Aldrich, 50% w/w in methanol) and silver hexafluoroantimonate (Alfa Aesar, 97%) were stored in an argon glovebox and were used without any further purification. Ethoxymethyl chloride (EMCl) (Aldrich, 95%) was dried over molecular sieves and subsequently over calcium hydride and then distilled just before use. 2,6-Di-*tert*-butylpyridine (DtBP) (Aldrich, ≥97.5%) was vacuum-distilled at 90 °C to remove any monosubstituted pyridine. High-purity argon was used to provide an inert atmosphere under which all reactions were carried out.

Synthesis of Initiator. The syntheses in situ of $C_2H_5OCH_2$-(THP)$^+[SbF_6]^-$ (ethoxymethyl-1-oxoniacyclohexane hexafluoroantimonate, EMOA) and $C_2H_5(OCH_2)^+[SbF_6]^-$ (ethyloxacarbenium hexafluoroantimonate, EOCA) were based on the reported synthesis described by Burgess et al.[47]

Preparation of EMOA Stock Solution. As an example, EMOA stock solution (16.45 mM) was prepared under argon in the

Scheme 2. Elementary Step Reactions Regulating the Pseudoequilibrium between Strain (A1) and Nonstrain (T1) Tertiary Active-Chain End Species in "Living" and Controlled CROP of Oxetane in THP

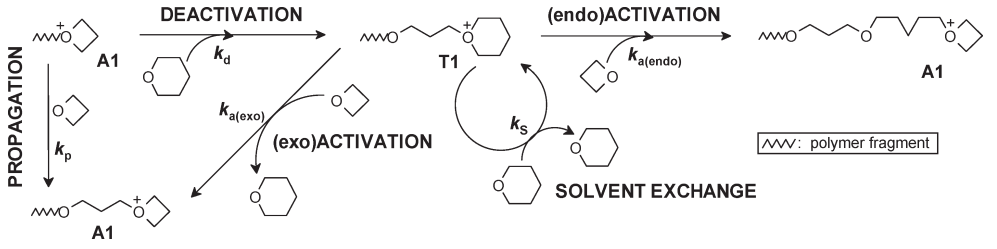

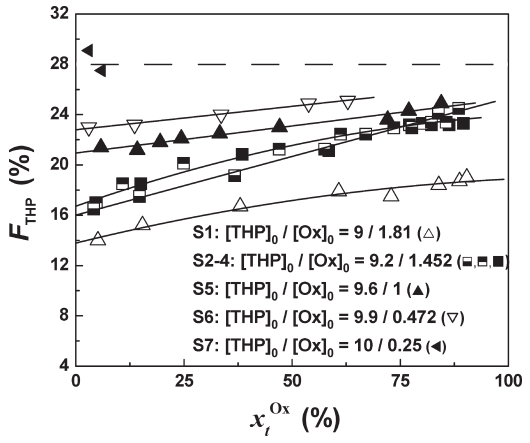

Figure 2. Cumulative copolymer composition in tetrahydropyran (F_{THP}) vs conversion in oxetane (x_t^{Ox}) dependences plotted at various initial molar fraction of oxetane (f_{Ox}), for the bulk copolymerization of oxetane (Ox) with tetrahydropyran (THP) at 35 °C initiated by (▲) $(BF_3{:}CH_3OH)_{THP}$ or by (▽, tilted ▲, ⬒, ⬓, ■, △) $C_2H_5OCH_2Cl/AgSbF_6$ in the presence of 2,6-di-*tert*-butylpyridine (DitBP) ([EMCl]/[$AgSbF_6$]/[DtBP] 1/1.1/1.1). Experiments: S1 (f_{Ox} = 0.167 44, $[EMCl]_0$ = 1.115 mM) (△); S2 (f_{Ox} = 0.1363, $[EMCl]_0$ = 1.115 mM) (■); S3 (f_{Ox} = 0.1363, $[EMCl]_0$ = 0.5 mM) (⬓); S4 (f_{Ox} = 0.1363, $[EMCl]_0$ = 2.3 mM) (⬒); S5 (f_{Ox} = 0.094 35, $[BF_3{:}CH_3OH]_0$ = 0.77 mM) (▲); S6 (f_{Ox} = 0.046 15, $[EMCl]_0$ = 1.115 mM) (▽); S7 (f_{Ox} = 0.0123, $[EMCl]_0$ = 1.115 mM) (tilted ▲). For additional experimental data, see Tables S1−S3 (series S1−S7) in Supporting Information.

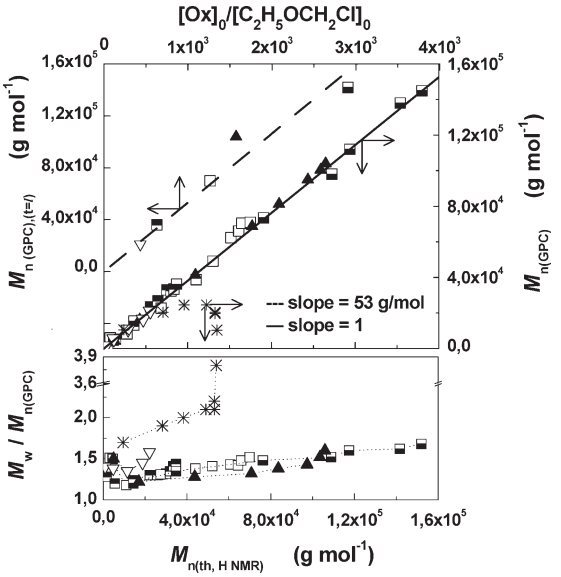

Figure 3. (i) Number-average molecular weight ($M_{n(GPC)}$) and molecular weight distribution ($M_w/M_{n(GPC)}$) vs $M_{n(th)}$ (= $[Ox]_0/[EMCl]_0$-($M_{Ox} + F_{THP}M_{THP}$)x_t^{Ox}) dependences. (ii) Number-average molecular weight at the "equilibrium" ($M_{n(GPC),(t=l)}$) vs $[Ox]_0/[EMCl]_0$ dependence, for the oxetane (Ox) polymerization initiated by $C_2H_5OCH_2Cl/AgSbF_6$ in the presence of 2,6-di-*tert*-butylpyridine (DtBP) ([EMCl]/[$AgSbF_6$]/[DtBP] 1/1.1/1.1 (n/n/n)) in (∗) dichloromethane (DCM) and in (⬒, ⬓, □, ▲, ▽) tetrahydropyran (THP) at various initial molar fraction of oxetane (f_{Ox}) at 35 °C. The conversion in oxetane (x_t^{Ox}) and composition of copolymer in THP (F_{THF}) were detrmined by ^{1}H NMR. Experiments: S1 (f_{Ox} = 0.167 44, $[Ox]_0$ = 1.81 M, $[EMCl]_0$ = 1.115 mM) (▲); S2 (f_{Ox} = 0.1363, $[Ox]_0$ = 1.452 M, $[EMCl]_0$ = 1.115 mM) (□); S3 (f_{Ox} = 0.1363, $[Ox]_0$ = 1.452 M, $[EMCl]_0$ = 0.5 mM) (⬓); S4 (f_{Ox} = 0.1363, $[Ox]_0$ = 1.452 M, $[EMCl]_0$ = 2.3 mM) (⬒); S6 (f_{Ox} = 0.046 15, $[Ox]_0$ = 0.479 M, $[EMCl]_0$ = 1.115 mM) (▽); S8 (f_{Ox} = 1, $[Ox]_0$ = 1.21 M, $[EMCl]_0$ = 1.115 mM)[39] (∗). Straight line indicates the M_n assuming that one polymer chain forms per molecule of initiators. The dotted straight line represents the linear regression for the M_n's at the "equilibrium" ($81 < x_{t=l}^{Ox} < 85\%$). For additional experimental data, see Tables S1−S3 (series S1−4,6) in Supporting Information.

glovebox, the flask protected from the light, by reaction of $AgSbF_6$ (373 mg, 1085 μmol) with EMCl (93 mg, 978 μmol), and 60 mL of THP used as solvent. The colorless mixture was stirred for at least 3 h at room temperature; AgBr precipitated immediately. Because tertiary 1-oxoniacyclohexane salts (or tetrahydropyranium salts) cannot be prepared under rigorous exclusion of moisture, ∼1.1 mol equiv of DtBP (240 μL, 1085 μmol) was used as a non-nucleophilic proton trap in order to neutralize the acid produced during the reaction between cationic species and the traces of water.[48]

Preparation of EOCA Stock Solution. The preparation of 60 mL stock solution of EOCA (16.4 mM) by the reaction of 968 μmol of EMCl (91.5 mg) and 1065 μmol of $AgSbF_6$ (366 mg) in the presence of 1065 μmol of DtBP (240 μL) was identical to the preparation of EMOA, except that DCM was used as solvent instead of THP.

Preparation of $BF_3{:}CH_3OH$ Stock Solution. A 60 mL stock solution of $BF_3{\cdot}CH_3OH$ (109 mM) in DCM or THP was prepared in the glovebox.

Polymerization Procedure. All polymerizations were carried out, as described in our previous article,[38,39] under a dry argon atmosphere in a glass calorimeter reactor[39] equipped with a magnetic stirrer and fitted with greaseless Rotaflo stopcocks. The reactor was previously flamed under vacuum. Then, a 50 mL solution of Ox in THP or in DCM was introduced under vacuum through the connected monomer storage flask. The water from the thermostat bath at 35 °C was continually passed through the outer double jacket. When the system was balanced to 35 °C, 3.8 mL of stock catalyst solution was injected into the calorimeter by means of a bleed valve system. After a proper interval, samples of the polymerizating solution were taken using an anaerobic sampling technique and then quenched by a solution of 10^{-2} M sodium hydroxide in water. The quenched reaction mixture was extracted with DCM and sequentially washed with water to neutralize the pH and to remove the initiator residues and salts. The DCM sample containing the polymer was then dried over $MgSO_4$. The dried polymer solution was filtered and the filtrate washed with dry DCM. The polymer was recovered from the organic layer by removal of the solvent to constant weight. The polymer yield ($wgt_{(polymer)}$) was determined gravimetrically, and the conversion in Ox (x^{Ox}) was calculated from the THP copolymer composition in mole (F_{THP}) and weight (G_{THP}) percent. As an example, the results obtained with

$[Ox]_0 = 1.452$ M, $[THP]_0 = 9.2$ M, $[EMOA]_0 = 1.115$ mM, and $[DtBP]_0 = 1.125$ mM were as follows: $x^{Ox}_{\sim 19h} = 80.1\%$, $F_{THP} = 23.3\%$, $M_{n(GPC)} = 70\,500$ g mol^{-1}, and $M_w/M_n = 1.42$ (sample S2.8, Table S1 in Supporting Information).

Kinetic Studies with EMOA Initiating System. This study was carried out as described above by adding the reagents in the following order: Ox ($50 - x$ mL, 1.947 M in THP), THP (x mL), and EMOA (3.8 mL, EMCl/$AgSbF_6$/DtBP 1/1.1/1.1 (n/n/n) in THP) for a total volume of polymerization of 53.8 mL. In the copolymerization experiments carried out with 1.115 mM of EMOA (3.8 mL, 15.8 mM in THP), 0, 9.9, 22.4, 37, and 43.1 mL of THP were respectively added to the Ox stock solution (1.947 M, in THP solvent) to attain an initial concentration in Ox (THP) of 1.81 (9), 1.452 (9.2), 1 (9.6), 0.472 (9.9), and 0.25 (20) M, respectively. Similarly, the copolymerization of 1.452 M of Ox with 9.2 M of THP (40.1 mL, 1.947 M in THP) by 0.5, 1.115, or 2.3 mM of EMOA was carried out by subsequent addition of 9.9 mL of THP and 3.6 mL of an EMOA stock solution of 32.5, 15.8, or 7.1 M, respectively.

Incremental Monomer Addition Technique. As an example chain extension polymerization in THP was carried out as described in the Polymerization Procedure section using 25 mL of 9/1 v/v Ox/THP mixture (1.545 M in THP) and 1.9 mL of EMOA stock solution in THP (60 mL, 16.45 mM in THP) containing of DtBP (240 μL, 17.1 mM). The initial concentrations were $[Ox]_0 = 1.452$ M, $[THP]_0 = 9.2$ M, $[EMOA]_0 = 1.115$ mM (i.e., $[EMCl]_0/[AgSbF_6]_0 = 1.1$), and $[DtBP]_0 = 1.227$ mM. After 19 and 21 h an aliquot of $\sim$1 mL was taken using the anaerobic sampling technique (e.g., $x^{Ox}_{21h} = 84\%$, $M_n = 73\,150$ g mol^{-1}, and $M_w/M_n = 1.36$) followed by the addition of 3 mL of a monomer stock solution (7 mL, 11.1 M) containing of DtBP (10 μL, 6.7 mM); $x^{Ox}_{21+14h} = 158\%$, $M_n = 154\,300$ g mol^{-1}, and $M_w/M_n = 1.41$. For additional experimental data see Figure 4.

Measurements. The copolymer compositions and microstructures were determined from ^{1}H and ^{13}C NMR spectra, which were obtained on a Bruker AC 300 spectrometer operating at 300.13 MHz for ^{1}H and 75.97 MHz for ^{13}C. $CDCl_3$ (Cambridge Isotope Lab. Inc.) was used as the solvent with TMS ($\delta = 0.00$ ppm) and $CDCl_3$ ($\delta = 77.0$ ppm) used as internal reference for ^{1}H and ^{13}C spectra.

Gel permeation chromatography (GPC) was performed on a Knauer instrument equipped with a Waters model 510 HPLC pump, a differential refractometer as detector, and two gel columns (supplied by Polymer Laboratories) used in series, 5 μ-PL gel columns with exclusion limits of 10^3 Å, and a mixed B column. Tetrahydrofuran (THF) was used as eluent at a flow rate of 1.0 mL min^{-1}. The measurements were carried out at ambient temperature, and the average molecular weights (M_n and M_w) were derived from a calibration curve based on polystyrene standards (600 to 10^6 g mol^{-1}). From the measured absolute molecular weight, this calibration leads to an error below 5%, which is an acceptable range for GPC analysis, when the value obtained for poly(oxetane-*co*-tetrahydropyran) is multiplied by a factor of $\sim$0.8. The absolute molecular weights were measured using a Waters HPLC system equipped with a model 515 pump, a model 2410 differential refractometer, an online 18-angle laser light scattering (MALLS) detector (DAWN DSP, Wyatt Technology Inc.), and three GPC TOSOH Bioscience polystyrene columns connected in the following series: TSK. Gel G-5000HXL, 4000HXL, and 3000HXL. The columns used separate polymers in the molecular weight range between $\sim 10^3$ and 10^6 g mol^{-1} with high resolution. THF (Aldrich) was used as an eluent at a flow rate of 1.0 mL min^{-1} at room temperature. The measurements were performed at room temperature. Data acquisition was performed using ASTRA version 4.81 software. The instruments were calibrated using narrow molecular weight polystyrene standards. The dn/dc of pseudoperiodic poly(oxetane$_{0.76}$-*co*-tetrahydropyran$_{0.24}$) solutions in THF was determined to be 0.0654 mL g^{-1} at 650 nm in THF at 25 °C using a differential refractometer.

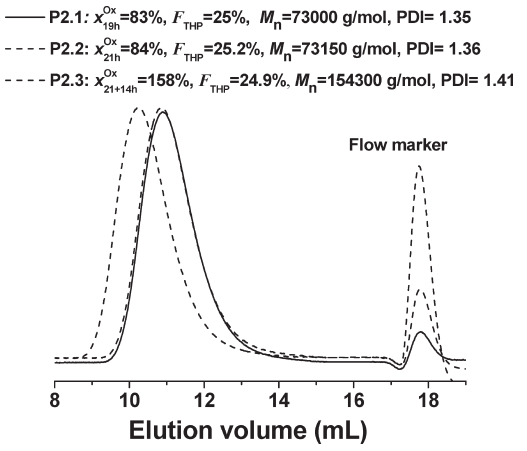

Figure 4. GPC RI traces of the original poly(oxetane-*co*-tetrahydropyran) (P2.1 and subsequently P2.2) and poly(oxetane-*co*-tetrahydropyran) (P2.3) obtained after the incremental monomer addition experiments in bulk for a initial molar fraction of oxetane (f_{Ox}) of 0.1363 at 35 °C with $C_2H_5OCH_2Cl/AgSbF_6$ as initiating system in the presence of 2,6-di-*tert*-butylpyridine (DtBP). Experimental conditions: [EMCl] = 1.115 mmol L^{-1}, $[AgSbF_6] = 1.17$ mmol L^{-1}, [DtBP] = 1.17 mmol L^{-1} and $[Ox]_{P2.1} = [Ox]_{P2.3} = 1.452$ mol L^{-1}.

Differential scanning calorimetry (DSC) measurements of poly(oxetane) and pseudoperiodic poly(oxetane$_{0.76}$-*co*-tetrahydropyran$_{0.24}$) were performed using a DSC Q 100, TA Instruments (UMD) over temperature range from −110 to 100 °C at the heating and cooling temperature of 10 °C min^{-1}. Both temperature and heat flow were calibrated with ultrapure indium. The glass transition temperature (T_g) was calculated using the inflection tangent as a method in determining the midpoint between the onset and the end of the step/glass transition region. The melting point, T_m is determined by the temperature at the maximum in the (dH/dT) plot near this transition. Data acquisition was performed using Rheology Advantage Data analysis version 5.1.42 software.

Results and Discussion

1. Structural Analysis. The copolymerization of THP (which has no homopolymerizability) with Ox was demonstrated by 300 MHz ^{1}H NMR spectroscopy. The ^{1}H NMR ($CDCl_3$, δ ppm) are as followed: 3.47 (t,−OCH_2− in Ox), 1.81 (m, −CH_2− in Ox), 3.39 (t, −OCH_2CH_2CH_2CH$_2$-CH_2O− in THP), 1.57 (p, −OCH$_2$CH_2CH_2CH_2CH$_2$O− in THP), 1.37 (p, −OCH$_2$CH$_2$CH_2CH$_2$CH$_2$O− in THP). The triplet at δ 3.46 ppm of similar intensity of the triplet at δ 3.39 was ascribed to the OCH_2 group of the oxetane fragment shifted from 3.47 ppm due to the presence of the THP fragment in the polymer. The 300 MHz ^{1}H NMR spectra of polymer obtained are shown in Figures S1 and S2 in the Supporting Information. Similar results were reported by Furukawa in the particular case of the copolymerization of THP with 3,3-bis(chloromethyl)oxetane.[49]

More structural details obtained by 75 MHz ^{13}C NMR spectrum (Figures S3 and S4 in Supporting Information) showed that each pentamethylene oxide fragment inserted into the polymer was flanked by two trimethylene oxide fragments. Indeed, in addition to the peaks at δ 67.86 and 30.09 ppm assigned to the −OCH$_2$CH$_2$$CH_2$O− and −OC-H$_2$$CH_2CH_2$O− groups, respectively, peaks at δ 22.79, 29.55, and 70.87 ppm were assigned to −OCH$_2$CH$_2$CH$_2$CH$_2$-CH$_2$O−, −OCH$_2$$CH_2CH_2$$CH_2CH_2$O−, and OCH$_2CH_2$-$CH_2CH_2CH_2$O− groups, respectively. The peak at δ 67.82 and 67.80 ppm of similar intensity as the peak at δ 70.97 was ascribed to OCH_2 group of the oxetane fragment shifted

Table 1. T_g (Glass Transition Temperature), T_m (Melting Temperature), and T_c (Crystallization Temperature) of Poly(oxetane-*co*-1,4-dioxane)[39] and Poly(oxetane-*co*-tetrahydropyran) Observed by Differential Scanning Calorimetry (Second Heating) at the Heating and Cooling Temperature of 10 °C min^{-1}

polymers	F_{Ox}, %	$M_{n(SEC)}$, g mol^{-1} (PDI)	T_g, °C	T_c peak, °C ($-\Delta H_C$, J g^{-1})	T_m peak, °C (ΔH_f, J g^{-1})
poly(Ox-*co*-1,4-D)[a]	98	~51 700 (1.22)	−80.9	−47 (25.6)	18 (70.1)
poly(Ox-*co*-THP)[b]	86	~41 000 (1.28)	−76.0	−33.7 (43.1)	−8.3 (41.7)
poly(Ox-*co*-THP)[c]	75	~33 430 (1.4)	−72.2	none	none

[a] The DSC thermogram is shown in Figures S7.3 in Supporting Information. [b] The DSC thermogram is shown in Figures S7.1 in Supporting Information. [c] The DSC thermogram is shown in Figures S7.2 in Supporting Information.

from 67.86 ppm due to the presence of the THP fragment in the polymer. Similarly, the peak at 30.06 ppm of similar intensity of the peak at 67.80 ppm is assigned to $-OCH_2-CH_2CH_2O-$ group shifted from 30.09 ppm due to presence of THP fragment.

Knowing by gravimetric measurement the polymer yield ($wgt_{(polymer)}$) and, by comparison of the integral values of the $-CH_2-$ peaks centered at 1.57, 1.37, and 1.81 ppm, the copolymer composition in THP fragment in mole (F_{THP}) and in weight (G_{THP}) percent, the conversion in Ox (x_t^{Ox}) and in THP (x_t^{THP}) as well as the $M_{n(th)}$ (theoretical number-average molecular weight calculated by ^{1}H NMR for 100% initiator efficiency) were calculated using eqs 1, 2, and 3, respectively.

$$x_t^{Ox} = 1 - [Ox]/[Ox]_0 = wgt_{(polymer)}/wgt_{(Ox)} \times (1 - G_{THP}) \quad (1)$$

$$x_t^{THP} = 1 - [THP]/[THP]_0 = wgt_{(polymer)}/wgt_{(THP)} \times G_{THP} \quad (2)$$

$$M_{n(th)} = \frac{[Ox]_0}{[initiator]_0} \times (M_{Ox} + F_{THP} \times M_{THP}) \times x_t^{Ox} \quad (3)$$

In Figure 2, the copolymer composition (F_{THP}) time dependences with varying the monomer feed ratio shows an apparent limited value noted $(F_{THP})_{(max)} \sim 28-30\%$ that cannot be exceeded at $f_{THP}/f_{Ox} > 9.98/0.25$. The 300 MHz ^{1}H NMR spectrum of polymer obtained at $f_{Ox} = 0.0244$ is shown in Figure S2 in the Supporting Information. Here, the failure in yielding copolymers with alternating microstructure (i.e., $F_{THP} = 0.5$) at 35 °C is an indication of the coexistence of both (endo)activation (i.e., copolymerization) and (exo)activation of T1 with propagation of A1.

DSC. Further studies using differential scanning calorimetry (DSC) showed that the incorporation of oxapentamethylene fragment in polyoxetane backbone profoundly influences the crystallization of the resulting copolymers. The thermogram of poly(oxetane-*co*-tetrahydropyran) of ~40 kg mol^{-1} (sample S1.3, Figure S7.1 in Supporting Information) shows at $F_{THP} = 14\%$ a cold crystallization starting at −33 °C immediately preceding a melting endotherm at −8 °C, which is 25 °C below the melting temperature of polyoxetanes (Figure 7.3 in Supporting Information) synthesized either in DCM or in 1,4-D, whereas a F_{THP} of 25% prevents the crystallization of copolymers of 33 kg mol^{-1} (sample S3.8, Figure S7.2 in Supporting Information). The transition temperature and the melting endotherm are compiled in the Table 1.

2. "Living" and Controlled CROP of Ox with THP Initiated by Ethoxymethyl-1-oxoniacyclohexane. Molecular Weight Control Free of Cyclic Oligomers. When the copolymerization of Ox with THP was carried out, either at various monomer feed ratio ($[THP]_0/[Ox]_0 = 9.9/0.472$, 9.6/1, 9.2/1.454, 9/1.81) using 1.115 mM EMOA ($[AgSbF_6]_0/[EMCl]_0 = 1.1$ in THP) or at various targeted DP_n in Ox (= $[Ox]_0/[EMCl]_0 = 630$, 1265, 2520) for a feed ratio $[THP]_0/[Ox]_0 = 9.2/1.454$, in the presence of DtBP as non-nucleophilic proton trap ($[DtBP]_0/[EMCl]_0 = 1.1$), the cyclic oligomers formation was prevented and the $M_{n(GPC)}$'s of the resulting polymers (Figure 3) showed, throughout the polymerization process, a value close to $M_{n(th)}$ (a theoretical number-average molecular weight calculated according to the eq 3 for 100% initiator efficiency). Since the process of chains growth involve competition reaction between solvent exchange reaction (i.e., T1 + THP $\rightarrow^{k_s}$ T1 + THP), (endo)activation (i.e., T1 + Ox $\rightarrow^{k_{a(endo)}}$ A1), and thus (exo)activation (i.e., T1 + Ox $\rightarrow^{k_{a(exo)}}$ A1 + THP), the conversion in Ox and the molecular weight reach a limited value noted x_l^{Ox} (i.e., limited monomer-to-polymer conversion in Ox) and $M_{n(l)}$ (i.e., number-average molecular weight at x_l^{Ox}), respectively, from which extending the time of polymerization (e.g., series P2: $[Ox]_0 = 1.454$ M, $[THP]_0 = 9.2$ M, $[EMCl]_0 = 1.115$ mM, $[AgSbF_6]_0 = 1.23$ mM, $[DtBP]_0 = 1.23$ mM; Figure 4) did not induce any significant redistribution of MWDs and any apparent decrease of the $M_{n(GPC)}$ as it is generally the case, in equilibrium polymerizations of oxolane,[7,8,19,20,50] presumably oxepane,[21] and more remarkably in the copolymerization of 1,3,5-trioxane with 1,3-dioxolane[51] or 1,3-dioxepane.[51,52] At x_l^{Ox} ($[Ox]_l \sim 0.19-0.14$ M), the linear dependence of $M_{n(l)}$ vs $[Ox]_0/[EMOA]_0$ (Figure 3) strongly indicates that process of chains growth reach a kind of state of "equilibration" in which the solvent exchange reaction (i.e., rate constant k_s, Scheme 2) compete substantially with reversible transfer (i.e., depropagation) and thus transfer to polymers (i.e., intra- and intermolecular transfer). In DCM, the polymerization of 1.452 M of oxetane initiated by 1.14 mM of EOCA ($C_2H_5(OCH_2)^+,[SbF_6]^-$) in the presence 1.22 mM DtBP is uncontrolled, leading to the production of linear polymer of $M_{n(GPC)} < M_{n(th,HNMR)}$ (Figure 3) together with the formation of cyclic oligomers (~5% of monomer consumed).[39]

The living nature of the chain end (sample P2.2, Figure 4) at x_l^{Ox} was demonstrated by chain extension polymerization, also known as incremental monomer addition technique. In this technique 3 mL of a new feed of Ox in THP ($[Ox]_0 = 11.1$ M) was added to the 24.9 mL of polymerization system under stirring. In Figure 4, the GPC RI traces of the original polymer at x_l^{Ox} and the polymer obtained after the incremental monomer addition show that $M_{n(GPC)}$ increases correspondingly from 73 150 g mol^{-1} (sample P2.2: $x_{21h}^{Ox} = 84\%$, $F_{21h}^{THP} = 25.2\%$, and $M_{n,th} = 69\,000$ g/mol) to 154 300 g mol^{-1} (sample P2.3); after that, ~80% of the added monomer was consumed (i.e., $M_{n(th)} = 145\,000$ g mol^{-1}). Here, the MWDs ($1.28 < PDI < 1.5-1.8$) of the resulting polymers are broader than predicted by the Poison distribution (MWDs $> 1 + 1/DP_n$), which we believe is due to a slow process of mutual conversion between A1 and T1. It cannot be excluded that the control over MWDs might be additionally affected by the dissociation in THP of the tight ion pairs into less stereoselective loose ion pairs and/or eventually free ions, providing free ions and ions pairs have different reactivities.[20]

3. Controlled CROP of Ox with THP initiated by BF_3CH_3OH. Molecular Weight Control Together with Cyclic Oligomers Formation. Using 7.7 mM $BF_3 \cdot CH_3OH$ for the

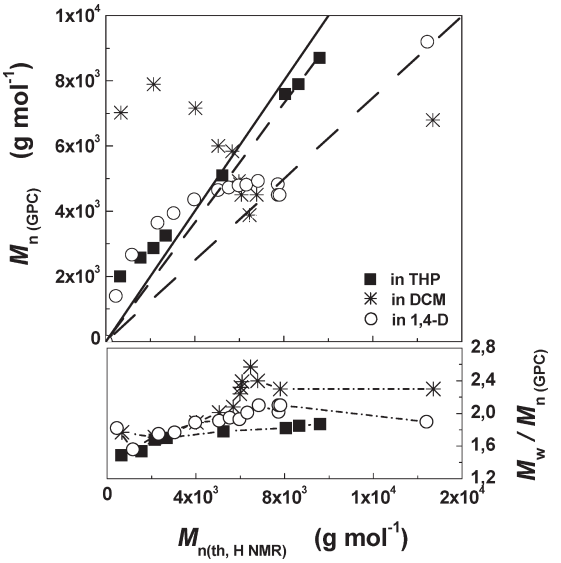

Figure 5. Number-average molecular weight ($M_{n(GPC)}$) and molecular weight distribution ($M_w/M_{n(GPC)}$) vs theoretical M_n's for the polymerization of 1 M of oxetane (Ox) initiated by 7.7 mM BF_3:CH_3OH in (∗) dichloromethane (DCM),[39] (○) in 1,4-dioxane $[1,4\text{-D}]_0/[Ox]_0 = 9$,[39] and in (■) in tetrahydropyran [THP]/[Ox] = 9.6 at 35 °C. For additional experimental details see Table 1 in the Supporting Information. The full straight line indicates the M_n assuming that one polymer chain forms per molecule of initiators, whereas the dotted straight lines are the linear regression for the experimental data. For additional experimental data, see GPC traces (Figure S9) and Table S3 (series S5) in the Supporting Information.

polymerization of 1 M Ox ($[THP]_0 = 9.6$ M), the dependence $M_{n(GPC)}$ vs $M_{n(th)}$ (Figure 5) and GPC traces (Figure S9 in Supporting Information) showed the attribute of a controlled polymerization process characterized by a slow initiation process. At $x^{Ox} = 47\%$ (sample P5.4), the $M_{n(GPC)}$ are somewhat lower than predicted by eq 3, and the formation of cyclic oligomers observed by ^{13}C NMR (~3−5% of the polymerized Ox at $x^{Ox} = 82\%$) demonstrates the existence of transfer reactions. In 1,4-D, more cyclic oligomers (~9% of the polymerized Ox at $x^{Ox} = 77.6\%$)[39] are formed, and $M_{n(GPC)}$ are lower than those obtained in THP, indicating that THP which is more nucleophilic than 1,4-D compete more efficiently with intramolecular transfer reactions, in particular with end-biting reactions. The ^{13}C NMR ($CDCl_3$, δ ppm) in cyclic oligomers are as follows: 1.81 (q, 2H, $-OCH_2CH_2CH_2O-$), 3.48 (t, 4H, $-OCH_2CH_2CH_2O-$, $DP_n > 4$), 3.54 (t, 4H, $-OCH_2CH_2CH_2O-$, $DP_n \leq 4$). ^{13}C NMR ($CDCl_3$, δ pm): 30.15 (s, $-OCH_2CH_2CH_2O-$), 67.08 and 67.44 (s, $-OCH_2CH_2CH_2O-$, $DP_n > 4$), 66.07 (s, $-OCH_2CH_2CH_2O-$, $DP_n \leq 4$). The 300 MHz ^1H NMR spectra of polymer obtained are shown in Figure S5 in the Supporting Information. Like the polymerization of oxetane in 1,4-D,[39] additional peaks of the main in-chain $-OCH_2CH_2CH_2O-$ and $-OCHH_2CH_2CH_2O-$ groups in cyclic oligomers were observed, indicating the presence of pentamethylene oxide units in cyclic oligomers.

4. Kinetics Studies. This studies was focused on data obtained in copolymerization of Ox with THP initiated with EMOA, conditions under which the process exhibit characteristics of a "living" and controlled polymerization process which implies linear dependences $M_{n(GPC)}$ vs $M_{n(th)}$ with no cyclic oligomers formation.

Dependences of the Overall Polymerization Rate on [EMOA], [Ox], and [THP]. From the elementary step reactions regulating the rate of mutual conversion between strained tertiary 1-oxoniacyclobutane (A1) and nonstrained (T1) tertiary 1-oxoniacyclohexane (Scheme 2), it was possible to express the overall rates of monomer consumption of Ox and THP as given by eqs 4 and 5, respectively.

$$-\frac{d}{dt}[Ox] = k_{Ox}^{app} \times [Ox] = (k_p^{app} + k_{a(endo)}^{app} + k_{a(exo)}^{app}) \times [Ox] \quad (4)$$

$$-\frac{d}{dt}[THP] = k_{THP}^{app} \times [Ox] = k_{a(endo)}^{app} \times [Ox] \quad (5)$$

with

$$k_a^{app} = k_{a(endo)}^{app} + k_{a(exo)}^{app} = (k_{a(endo)} + k_{a(exo)}) \times P_{aT1,t} \times [T1] \quad (6)$$

and

$$k_p^{app} = k_{a(endo)} \times [T1] \quad (7)$$

where k_{Ox}^{app} (s^{-1}), k_p^{app} (s^{-1}), k_d^{app} (s^{-1}), $k_{a(endo)}^{app}$ ($= k_{THP}^{app}$) (s^{-1}), and $k_{a(exo)}^{app}$ (s^{-1}) are the apparent rate constant of Ox consumption of A1 and T1, propagation of A1, deactivation of A1, (endo)activation of T1 (copolymerization of THP), and (exo)activation of T1, respectively, and k_p ($L\ mol^{-1}\ s^{-1}$), k_d ($L\ mol^{-1}\ s^{-1}$), $k_{a(endo)}$ ($L\ mol^{-1}\ s^{-1}$), and $k_{a(exo)}$ ($L\ mol^{-1}\ s^{-1}$) the corresponding rate constants. Here eq 5 predicts that the rate of THP consumption is kinetically controlled by the rate of (endo)activation of T1 (i.e., $k_{a(endo)}^{app} \times [Ox]$) rather than by the rate of deactivation of A1 (i.e., $k_d^{app} \times [THP]$) as THP can be regenerated from T1 by (exo)activation (i.e., $k_{a(exo)}^{app} \times [Ox]$). Because the solvent exchange reactions (i.e., $k_s^{app} \times [THP]$) suspend, at the "equilibration" (i.e., $[Ox]_l = 0.2-0.14$ M), the activation of T1 (i.e., $k_s^{app} \times [THP] \gg k_a^{app} \times [Ox]_l$) as well as reversible transfer (i.e., depropagation), our kinetics consideration predict that the overall apparent rate constant of activation (k_a^{app}), given by eq 6, is related to the solvent exchange reaction by

$$P_{aT1,t} = \frac{(k_{a(endo)} + k_{a(exo)}) \times ([Ox] - [Ox]_l)}{(k_{a(endo)} + k_{a(exo)}) \times ([Ox] - [Ox]_l) + k_s \times [THP]} \quad (8)$$

and

$$P_S = \frac{k_s}{k_{a(endo)} + k_{a(exo)}} \quad (9)$$

Here P_{aT1} ($0 \leq P_{aT1,t} < 1$) can be view as a factor of activation of T1 in the consideration of the existence of the solvent exchange reaction ($P_S \neq 0$), and P_S reads as a factor determining the inherent state of "equilibration". At the "equilibration" ($[Ox]_l = 0.2-0.14$ M), eq 8 reads $P_{aT1,l} \sim 0$. The integrations of eqs 4 and 5 and the combination of the resulting equations with eqs 1 and 2 give eqs 10 and 11

$$x_t^{THP} \times [THP]_0 = k_{THP}^{app} \times [Ox]_0 \times \int_0^t (1 - x_t^{Ox})\, dt \quad (10)$$

$$x_t^{Ox} \times [Ox]_0 = k_{Ox}^{app} \times [Ox]_0 \times \int_0^t (1 - x_t^{Ox})\, dt \quad (11)$$

From the value of the initial rate of monomers consumption given by the slope of the plots of the left-hand side of

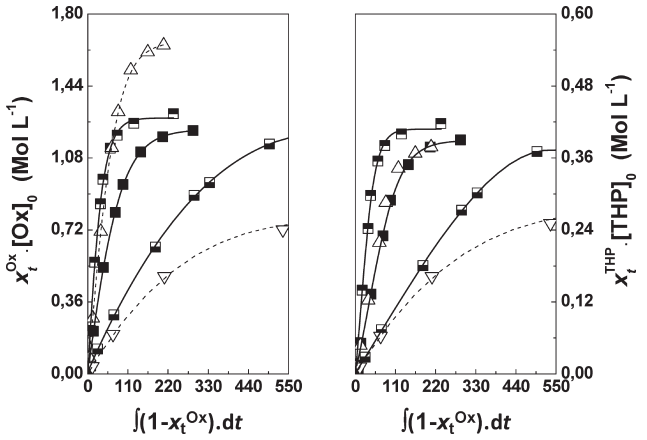

Figure 6. Evolution of $x_t^{THP}[THP]_0$ and $x_t^{Ox}[Ox]_0$ vs $\int(1 - x_t^{Ox})\,dt$ for the oxetane (Ox) copolymerization with tetrahydropyran (THP) initiated by $C_2H_5OCH_2Cl/AgSbF_6$ in the presence of 2,6-di-*tert*-butylpyridine (DtBP) ([EMCl]/[$AgSbF_6$]/[DtBP] 1/1.1/1.1) at various initial molar fraction of oxetane (f_{Ox}) at 35 °C. $x_t^{THP}(1 - [THP]/[THP]_0)$ and $x_t^{Ox}(1 - [Ox]/[Ox]_0)$ were calculated from ^{1}H NMR. Experiments: S1 (f_{Ox} = 0.167 44, [EMCl]$_0$ = 1.115 mM) (△); S2 (f_{Ox} = 0.1363, [EMCl]$_0$ = 1.115 mM) (■); S3 (f_{Ox} = 0.1363, [EMCl]$_0$ = 0.5 mM) (⬓); S4 (f_{Ox} = 0.1363, [EMCl]$_0$ = 2.3 mM) (⬒); S6 (f_{Ox} = 0.046 15, [EMCl]$_0$ = 1.115 mM) (▽). For additional experimental data, see Tables S1−S3 (series S1−4,6) in Supporting Information.

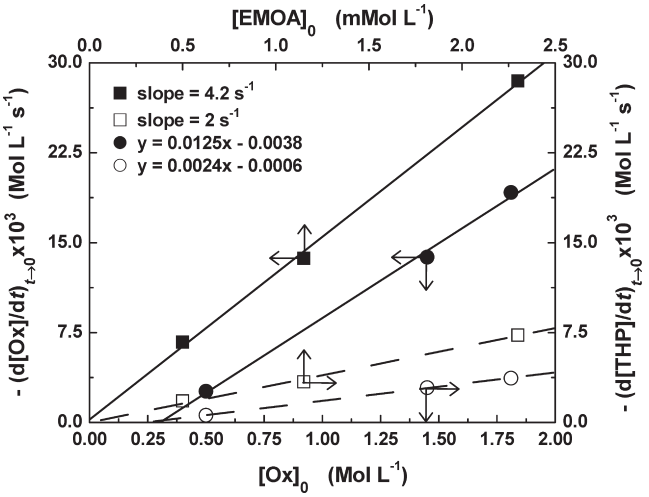

Figure 7. Initial rate of monomers consumption plotted against [Ox] at [EMCl] = 1.115 mM (●, ○) and against [EMCl] at [Ox] = 1.542 mM (■, □) for determining the order in oxetane (Ox) and in CH_2OCH_2Cl (EMCl), respectively, in the bulk copolymerization of oxetane (Ox) with tetrahydropyran (THP) initiated by EMCl/$AgSbF_6$ in the presence of 2,6-di-*tert*-butylpyridine (DtBP) ([EMCl]/[$AgSbF_6$]/[DtBP] = 1/1.1/1.1) at 35 °C. Experiments: S1 (f_{Ox} = 0.167 44, [EMCl]$_0$ = 1.115 mM); S2 (f_{Ox} = 0.1363, [EMCl]$_0$ = 1.115 mM); S3 (f_{Ox} = 0.1363, [EMCl]$_0$ = 0.5 mM); S4 (f_{Ox} = 0.1363, [EMCl]$_0$ = 2.3 mM); S6 (f_{Ox} = 0.046 15, [EMCl]$_0$ = 1.115 mM). For additional experimental data, see Tables S1−S3 (series S1−4,6) in Supporting Information.

eqs 10 and 11 vs $\int(1 - x_t^{Ox})\,dt$ (see Figure 6), it was then possible, as shown in Figure 7, to verify the first-order dependence on [Ox]$_0$ and on [EMOA]$_0$ of both eqs 4 and 5. For this purpose, the bulk copolymerization of oxetane with THP at 35 °C was studied using 1.15 mM EMOA (i.e., initiator yielding fast and instant initiation) for four different concentrations of oxetane (0.5, 1, 1.42, and 1.81 M) and using 1.452 M oxetane for three different concentrations of EMOA (0.5, 1.15, and 2.3 mM). In all experiments, EMOA was formed from EMCl/$AgSbF_6$ in THP in the presence of DtBP prior its addition to the monomer solution (∼15−30 min). In eqs 10 and 11, the integral value of $(1 - x_t^{Ox})$ was given by the graphical integration on the [Ox]$_t$/[Ox]$_0$−time curve using a second-order fit exponential regression (Figure S10 in Supporting Information). In Figure 6, the plot of the left side of eqs 10 and 11 vs $\int(1 - x_t^{Ox})\,dt$ gives, at all concentrations of EMOA and Ox, a quasi-straight line during the major part of the polymerization run (as long as [Ox]$_t$ > 0.3 M), indicating that the stationary state concentrations of A1 and T1 are reached at the fairly early stages of the polymerization, i.e.

$$-\frac{d[A1]}{dt} = \frac{d[T1]}{dt} = k_d \times [A1] \times [THP] - (k_{a(endo)} + k_{a(exo)}) \times P_{aT1} \times [T1] \times [Ox] = 0 \quad (12)$$

After rearrangement of eq 12, the activation−deactivation pseudoequilibrium coefficient (Q_t) which does not formally follow the principle of microscopic reversibility is given by eq 13.

$$Q_t = \frac{K_0}{P_{aT1}} \quad (13)$$

with

$$K_0 = \frac{k_d}{k_{a(endo)} + k_{a(exo)}} = \frac{[T1] \times [Ox]}{[A1] \times [THP]} \quad (14)$$

Here, K_0 is read as the activation−deactivation pseudoequilibrium constant in the consideration of $k_s = 0$ (i.e., $P_S = 0$ and $P_{aT1.t} = 1$). At the later stages of the polymerization, the decreases observed in Figure 6 for both $k_{a(endo)}^{app}$ and k_{Ox}^{app} ($= k_P^{app} + k_{a(endo)}^{app} + k_{a(exo)}^{app}$), namely, close to the "equilibration" (0.14−0.18 M < [Ox] < 0.3 M) indicates the inadequacy of the steady-state assumption (eq 12) on which eq 13 is based at [Ox] > 0.3−0.4 M. In Figure 7, the plot of the initial rate of Ox (i.e., $x_t^{Ox} \times [Ox]_0/\int(1 - x_t^{Ox})\,dt$) and THP (i.e., $x_t^{Ox} \times [THP]_0/\int(1 - x_t^{Ox})\,dt$) consumptions as a function of [EMOA] and [Ox] show, at this concentrations range, the first-order dependence on [EMOA] and on [Ox] as well as the existence of the "equilibration" from the intercept, by linear dependences $-d[Ox]/dt$ and $-d[THP]/dt$ vs [Ox], of the *X*-axis at approximately the limited monomer-to-polymer concentrations ([Ox]$_l$ = 0.2 M) where $P_{aT1,l} \sim 0$.

Determination of Reactivity Ratio k_p/k_d and $k_{a(endo)}/k_{a(exo)}$. By dividing eq 4 by eq 5 and combining the resulting equation with eqs 13 and 14, after rearrangement one obtains eq 15.

$$\frac{-d[Ox]/dt}{-d[THP]/dt} = \frac{r_{Ox}}{P_{a(endo)}} \times \frac{[Ox]}{[THP]} + \frac{1}{P_{a(endo)}} \quad (15)$$

with

$$r_{Ox} = \frac{k_p}{k_d} \quad (16)$$

and

$$P_{a(endo)} = \frac{k_{a(endo)}}{k_{a(endo)} + k_{a(exo)}} \quad (17)$$

where r_{Ox} is the monomer reactivity ratio for Ox and $P_{a(endo)}$ is the factor representing the contribution of (endo)activation to the overall activation process of T1. As illustrated in Figure 8, the plot on the left side of the eq 15 vs instant

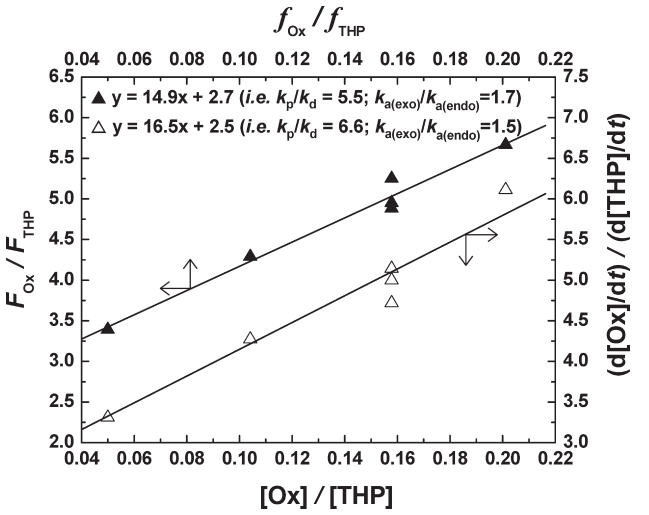

Figure 8. Copolymer composition ratio (F_{Ox}/F_{THP}) vs monomer feed ratio (f_{Ox}/f_{THP}) and relative reaction rate ($(-d[Ox]/dt)/(-d[THP]/dt)$) vs [Ox]/[THP] for the bulk copolymerization of oxetane (Ox) with tetrahydropyran (THP) initiated by EMCl/$AgSbF_6$ in the presence of 2,6-di-*tert*-butylpyridine (DtBP) ([EMCl]/[$AgSbF_6$]/[DtBP] = 1/1.1/1.1) at 35 °C. Experiments: S1 (f_{Ox} = 0.167 44, $[EMCl]_0$ = 1.115 mM); S2 (f_{Ox} = 0.1363, $[EMCl]_0$ = 1.115 mM); S3 (f_{Ox} = 0.1363, $[EMCl]_0$ = 0.5 mM) ; S4 (f_{Ox} = 0.1363, $[EMCl]_0$ = 2.3 mM); S6 (f_{Ox} = 0.046 15, $[EMCl]_0$ = 1.115 mM). For additional experimental data, see Tables S1−S3 (series S1−6) in Supporting Information.

monomer ratio [Ox]/[THP] yields a straight line, with the slope and the intercept of $r_{Ox}/P_{a(endo)}$ and $1/P_{a(endo)}$, respectively. Comparing the k_p/k_d and $k_{a(endo)}/k_{a(exo)}$ values determined from eq 15 and from the determination by ^{1}H NMR of the copolymer composition at various feed composition (eq 18), the agreement is quite reasonable. This shows that as long as k_{THP}^{app} is constant, there is no variation of the reactivity ratio with the change of the comonomer composition. The r_{Ox} and $P_{a(endo)}$ values determined from Figure 8 are listed in Table 2.

$$\frac{(F_{Ox})_{x^{Ox}<10\%}}{(F_{THP})_{x^{Ox}<10\%}} = \frac{1}{P_{a(endo)}} + \frac{r_{Ox}}{P_{a(endo)}} \times \frac{f_{Ox}}{f_{THP}} \qquad (18)$$

Determination of the Rate Constant Ratio $k_s/k_{a(endo)}$ and $k_s/k_{a(exo)}$. While the $x_t^{THP} \times [THP]_0$ vs $[Ox]_0 \times \int(1 - x_t^{Ox})\, dt$ plots shows the change of $k_{a(endo)}$ with conversion, after combination of eqs 5, 6, and 8 and rearrangement of the resulting equations, one obtains eq 19

$$\frac{[Ox]_0}{-d[THP]/dt} = \frac{1}{k_{a(endo),\,t\to 0}^{app}} + \frac{P_S}{k_{a(endo),\,t\to 0}^{app}} \times \frac{[THP]}{[Ox]-[Ox]_l} \qquad (19)$$

from which it was more advantageous, for the determination of the factor determining the inherent state of equilibration P_S (eq 9) to plot the reciprocal apparent rate constant of (endo)activation (i.e., copolymerization) extrapolated to zero time as a function of $[THP]/([Ox] - [Ox]_l)$ with the slope and the intercept of $1/k_{a(endo),t\to 0}^{app} \times P_S$ and $1/k_{a(endo),t\to 0}^{app}$, respectively. Here, $k_{a(endo),t\to 0}^{app}$ represents the value of $k_{a(endo)}$ extrapolated to zero time. For comparison, the identical values of $k_s/k_{a(endo)}$ obtained at various concentration of Ox and EMOA shows that the solvent exchange reaction can be predicted by our kinetic considerations and that $k_s/k_{a(endo)}$ is independent of the change of the of comonomer composition. It must be noted that the definition of eq 8, which shows a specific feature of the CROP kinetics of Ox with THP or 1,4-D,[38,39] is also found in mediated-RAFT polymerization,[53] in the process viewed as degenerative chain transfer reaction, for the understanding and the estimation of the magnitude of the exchange reaction (i.e., crossover efficiency) in the unsuccessful block copolymerization of styrene with methyl methacrylate,[54,55] in the induction[56] and rate retardation phenomena,[56−58] and in the formation of polymer with bimodal GPC distribution.[59−61] Similar development is also found in nitroxide-mediated controlled free radical batch emulsion polymerization, in the process view as compartmentalization of propagating radical, to discuss whether or not the overall rate of irreversible termination is reduced with respect to that in a similar bulk process.[62]

Determination of k_p, k_d, k_s, $k_{a(endo)}$, and $k_{a(exo)}$. According to Figure 7, the initial rate of living chains end growth is first-order dependence on [Ox] and [EMCl] (=[EMOA]). Considering the terminal model for the chains growth, the expression of the average binary copolymerization rate constant $\langle k_M \rangle$ is given by the general equation

$$\langle k_M \rangle = \frac{\langle k_M^{app} \rangle}{[EMOA]_0} = \frac{-d[Ox]/dt - d[THP]/dt}{[Ox] \times ([A1] + [T1])} \qquad (20)$$

Here $\langle k_M \rangle$, which is experimentally accessible (i.e., $[EMOA]_0 = [A1]+[T1]$), can then be expressed as a simple function of comonomer feed ratio instead of concentration of A1 and T1 by combining eqs 4, 5, 13, 14, and 20 and rearranging the resulting equation as given by eq 21.

$$\left(r_{Ox} + (1 + P_{a(endo)}) \times \frac{f_{THP}}{f_{Ox}}\right) \times \frac{[EMOA]_0}{\langle k_M^{app} \rangle} = \frac{1}{k_d} + \frac{Q_t}{k_d} \times \frac{f_{THP}}{f_{Ox}} \qquad (21)$$

The values of k_d and Q_t calculated from the intercept and the slope, respectively, of the plot of left side of eq 21 vs f_{THP}/f_{Ox} (Figure 10) were used, by mean of the reactivity ratio r_{Ox} (eq 16), $P_{a(endo)}$ (eq 17), and P_S (eq 9), to calculate the rate constant of reactions involved in the living cationic ring-opening copolymerization of Ox with THP (see Scheme 2). In this study, the two series of values obtained for k_p, k_d, k_s, $k_{a(endo)}$, and $k_{a(exo)}$ are based on either k_p/k_d and k_s determined from the kinetic data obtained using eq 15 or from the copolymer composition obtained using eq 18. The k_p values, 50 ± 5 L mol^{-1} s^{-1}, obtained in this study are in the range, even though 10-folder higher than that of the value calculated from the kinetics parameters describing, according to the transition state theory, the CROP of oxetane in DCM and methylcyclohexane at T ≤ −20 °C.[63] The data are listed in Table 3.

5. Copolymerization Model Fitting and Mechanistic Interpretation. Using concentrations of [THP] = 9.2 M and [Ox] = 1.452 M, the following time intervals (τ) between two consecutive events have been calculated at the early stages of the polymerization process.

$$11 \text{ ms (i)} < \tau_d = 1/(k_d \times [THP]_0) < 15.7 \text{ ms (ii)}$$

$$\tau_{a(exo)} = 1/(P_{aT1,\,t=0} \times k_{a(exo)} \times [Ox]_0) = 0.24 \text{ s}$$

$$\tau_{a(endo)} = 1/(P_{aT1,\,t=0} \times k_{a(endo)} \times [Ox]_0) = 0.41 \text{ s}$$

$$12.6 \text{ ms (i)} < \tau_p = 1/(k_p \times [THP]_0) < 15.3 \text{ ms (ii)}$$

$$\tau_s = 1/(k_s \times [THP]_0) = 3 \text{ s } (\tau_s = 1/((1 - P_{aT1,\,t=0}) \times k_s \times [THP]_0) = 57 \text{ s})$$

Table 2. Calculated Value for the Rate Constant of Solvent Exchange Reaction (k_S), the Factor Determining the Inherent State of "Equilibration" (P_S), and the Factor of Activation of T1 Extrapolated to Zero Time ($P_{a,T1,t\to0}$) for the Bulk CROP of Oxetane (Ox) with Tetrahydropyran (THP) at 35 °C

						k_S (L mol^{-1} s^{-1})	
series	$[THP]_0/[Ox]_0$ (mol L^{-1}/ mol L^{-1})	$[I]_0$ (mmol L^{-1})	$[Ox]_f$ (mol L^{-1})	P_S	$P_{a,T1,t\to0}$	from eq 15	from eq 18
S1[a]	9/1.81	1.115	0.167	0.005 32	0.971	0.0254	0.0255
S2[a]	9.2/1.454	1.115	0.193	0.007 66	0.947	0.0366	0.0367
S3[a]	9.2/1.454	2.3	0.159	0.006 37	0.956	0.0305	0.0306
S4[a]	9.2/1.454	0.5	0.166	0.006 43	0.966	0.0307	0.0308
S5[a]	9.9/0.5	1.115	0.172	0.005 36	0.849	0.0256	0.0257
S6[b]	9.6/1	7.7	0.187	0.007 44	0.919	0.0356	0.0357
					$<k_s>$ =	0.0307	0.0308

[a] With $C_2H_5OCH_2Cl$/AgSBF6/DtBP (1/1/1.05) initiating system ($[I]_0 = [C_2H_5OCH_2Cl]_0$). [b] With $(BF_3\cdot CH_2OH)_{THP}$ initiating system ($[I]_0 = [BF_3\cdot CH_2OH]_0$).

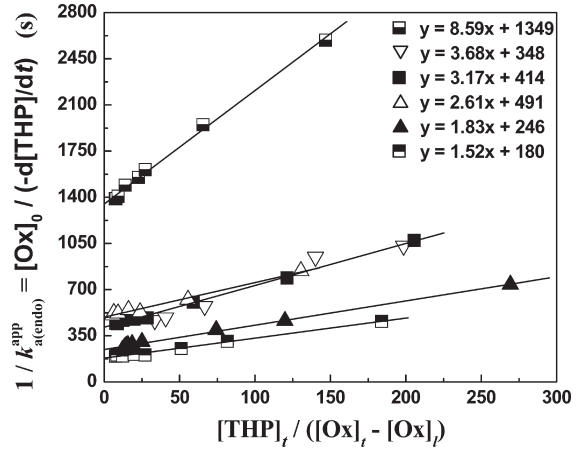

Figure 9. Plot of the reciprocal initial rate of (endo)activation vs $[THP]/([Ox]_0 - [Ox]_f)$ for the copolymerization of Ox with THP at 35 °C. Experiments: S1 (f_{Ox} = 0.167 44, $[EMCl]_0$ = 1.115 mM) (△); S2 (f_{Ox} = 0.1363, $[EMCl]_0$ = 1.115 mM) (■); S3 (f_{Ox} = 0.1363, $[EMCl]_0$ = 0.5 mM) (⬓); S4 (f_{Ox} = 0.1363, $[EMCl]_0$ = 2.3 mM) (⬒); S5 (f_{Ox} = 0.094 35, $[BF_3{:}CH_3OH]_0$ = 0.77 mM) (▲); S6 (f_{Ox} = 0.046 15, $[EMCl]_0$ = 1.115 mM) (▽). For additional experimental data, see Tables S1−S3 (series S1−6) in Supporting Information.

with

$$P_{aT1,\,t=0} = 0.947$$

Thus, the time interval between two activations is relatively long, 0.41 s by (endo)activation and 0.24 s by (exo)activation. At this stage, solvent exchange reactions does not suspend the process of activation as the time interval between two reactions is 3 s (57 s) ≫ 0.41 s. The tertiary 1-oxoniacyclobutane A1 stays active for a very short time, only 15.7 ms, before deactivation takes place, and the polymer end goes back to a kind of "dormant" state. At the early stages of the polymerization, 6.7% of the living ACE species bear the terminal group A1. Propagation is 0.87 times slower than deactivation, however monomer incorporates on average every 12.6 ms, and 9 monomer units are added after 10 active cycles. Similarly, the (exo)activation is 1.7 times faster than (endo)activation (copolymerization) and 10 Ox units and 4 THP units are added after 10 actives cycles. The number of monomer molecules added during first 10 active cycles is 18 Ox units and 4 THP units. Since the deactivation reaction is time-independent in the considered system ($[THP] \sim [THP]_0$ throughout the polymerization process), the number of monomer units added by cycle decreases with conversion. Figure 11 shows that the kinetics parameter obtained in this study provide a reasonable

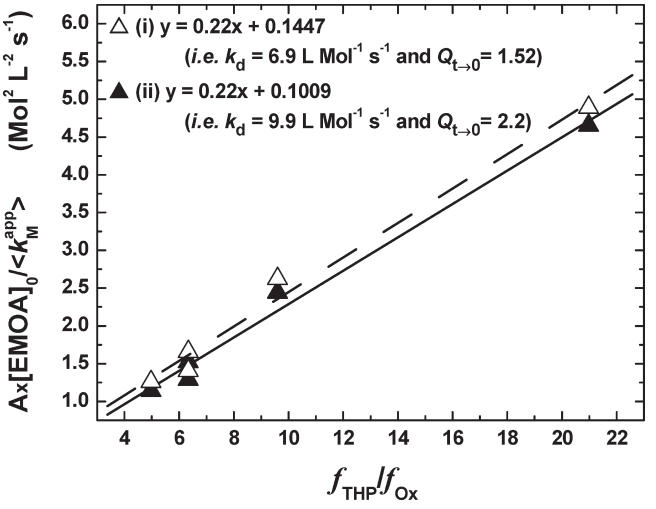

Figure 10. $A \times [EMOA]_0/\langle k_M^{app}\rangle$ vs monomer feed ratio (f_{Ox}/f_{THP}) (with $A = r_{Ox} + (1 + P_{a(endo)}) \times (f_{Ox}/f_{THP})$) for the bulk copolymerization of oxetane (Ox) with tetrahydropyran (THP) initiated by EMCl/$AgSbF_6$ in the presence of 2,6-di-*tert*-butylpyridine (DtBP) ($[EMCl]/[AgSbF_6]/[DtBP] = 1/1.1/1.1$) at 35 °C, using either the values of $\langle k_M^{app}\rangle$ calculated from the kinetics data (method i, eq 15) or from the copolymer composition data (method ii, eq 18). Experiments: S1 (f_{Ox} = 0.167 44, $[EMCl]_0$ = 1.115 mM); S2 (f_{Ox} = 0.1363, $[EMCl]_0$ = 1.115 mM); S3 (f_{Ox} = 0.1363, $[EMCl]_0$ = 0.5 mM); S4 (f_{Ox} = 0.1363, $[EMCl]_0$ = 2.3 mM); S6 (f_{Ox} = 0.046 15, $[EMCl]_0$ = 1.115 mM). For additional experimental data, see Tables S1−S3 (series S1−4,6) in Supporting Information.

fit with the $\langle k_M^{app}\rangle$ ($= k_{Ox}^{app} + k_{THP}^{app}$) and composition ($F_{Ox}$) data.

Conclusions

The living and controlled CROP of Ox in THP (with has no homopolymerizability) led readily to a copolymer chains with pseudoperiodic sequences and controlled molecular weight (up to 150 000 g/mol). The determination of the overall kinetic order of rate of monomers consumption as well as the dependence $M_{n(GPC)}$ vs conversion revealed the existence of a state of "equilibration" (i.e., T1 + THP $\rightarrow^{k_s}$ T1 + THP) at $[Ox]_f$ = 0.14−0.2 M from where, in the apparent absence of reversible transfer (i.e., T1 ↔ A1 + THP), no fall of the M_n's were recorded. The coexistence of the growing species in the form of strain ACE species (propagating chain terminated by a tertiary 1-oxoniacyclobutane ion, A1) and strain-free ACE species ("dormant" chain terminated by a tertiary 1-oxoniacyclohexane ion, T1) was demonstrated from the microstructures of the copolymers as each pentamethylene oxide fragment inserted into the polymer is flanked by two trimethylene oxide fragments, and thus deactivation

Table 3. Kinetic Parameters for the Bulk CROP of Oxetane (Ox) with Tetrahydropyran (THP) at 35 °C

parameters		value (from eq 15)	value (from eq 18)
r_{Ox} (= k_p/k_d)	monomer reactivity ratio for oxetane	6.6	5.5
$P_{a(endo)}$ (= $k_{a(endo)}/(k_{a(endo)} + k_{a(exo)})$)	factor of (endo)activation of T1	0.4	0.37
k_p (L mol^{-1} s^{-1})	rate constant of propagation of A1	45.4	54.5
k_d (L mol^{-1} s^{-1})	rate constant of deactivation of A1	6.9	9.9
$k_{a(endo)}$ (L mol^{-1} s^{-1})	rate constant of (endo)activation of T1	1.9	1.8
$k_{a(exo)}$ (L mol^{-1} s^{-1})	rate constant of (exo)activation of T1	2.9	3
K_0 (= $k_d/(k_{a(endo)} + k_{a(exo)})$)	ideal pseudoequilibrium constant (P_S = 0)[a]	1.44	2.07
$\langle k_s \rangle$ (L mol^{-1} s^{-1})	rate constant of solvent exchange reaction	0.0307	0.0308

[a] Factor determining the inherent state of "equilibration".

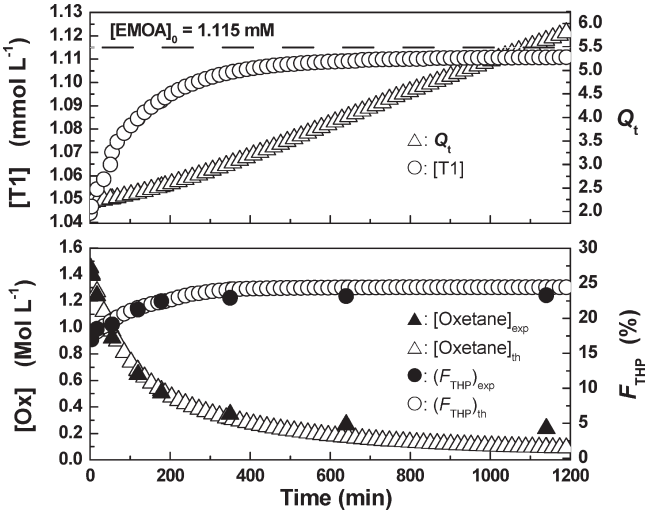

Figure 11. Predicted values of the copolymer composition in tetrahydropyran F_{THP} and of the activation−deactivation pseudoequilibrium coefficient Q_t together with the variation in concentrations of monomer [Ox] and of dormant species [T1] as a function of time in the bulk living copolymerization of oxetane (Ox) with tetrahydropyran (THP) initiated by EMCl/$AgSbF_6$ in the presence of 2,6-di-*tert*-butylpyridine (DtBP) ([EMCl]/[$AgSbF_6$]/[DtBP] = 1/1.1/1.1) at 35 °C. The open symbol represents the theoretical dependences based on the terminal model, and the closed symbol represents the experimental data. $[Ox]_0$ = 1.452 M, $[THP]_0$ = 9.2 M, $[EMCl]_0$ = 1.115 mM, $[DtBP]_0$ = 1.12 mM, and $[AgSbF_6]_0$ = 1.2 mM (series S2).

(A1 + THP $\rightarrow^{k_d}$ T1), activation (T1 + Ox $\rightarrow^{k_a}$ A1), and solvent exchange reaction (T1 + THP $\rightarrow^{k_s}$ T1 + THP) occur throughout the polymerization process. The activation−deactivation pseudoequilibrium coefficient Q_t and constant K_0 (= $Q_t \times P_{aT1,t}$) were determined in a pure theoretical basis, using the terminal model. Although there is appreciable uncertainty concerning the estimations of the k_s (~ $[Ox]_l$) for the strain-free ACE species T1, the kinetics parameters calculated in this study provide a reasonable fit with the measured apparent rate constant of monomers consumption (k_{Ox}^{app} and k_{THP}^{app}) and with the copolymer composition (F_{Ox}) data. The form of the pseudoequilibrium equation shows that Q_t is strictly dependent on $P_{aT1,t}$ ($1/P_{aT1,t} = 1 + k_s/k_a \times [THP]/([Ox] - [Ox]_l)$) and stay, even if it increases during the course of the copolymerization with [T1]/[A1], close to the lowest value K_0 (pseudoequilibrium constant in the consideration of k_s = 0), a state of mutual conversion in which macro tertiary oxonium ions are predominantly (~94%) in the "dormant" form T1. Although the occurrence of some extent of transfer cannot be excluded with appreciable uncertainty, the formation of polymer with large PDI (~1.4−1.8) are more likely to be the result of slow mutual conversion between of A1 and T1 with respect to chains growth (k_p/k_d ~ 5.4 and k_p/k_a ~ 11.3) than the cause of chain scission reactions.

Acknowledgment. This research was financially supported by QinetiQ, formerly Defence Evaluation and Research Agency. Special thanks to Ravin (Laurentian University) for providing time to complete this work and the LCPO (Université Bordeaux 1, ENSCPB) for the DSC analysis.

Supporting Information Available: 300 MHz ^{1}H and 75 MHz ^{13}C NMR spectrum (Figures S1(i) and S3(i)) of poly(oxetane) obtained in dichloromethane (DCM) with $[Ox]_0$ = 1 M, $[BF_3{:}CH_3OH]_0$ = 7.7 mM and conversion = 80.8% (sample P1.8, Table 1); 300 MHz ^{1}H and 75 MHz ^{13}C chemical shift in $CDCl_3$ of $-CH_2-$ groups in poly(oxetane) and poly(oxetane-*co*-tetrahydropyran) (Table S4); tables, GPC RI traces, 300 MHz ^{1}H and 75 MHz ^{13}C NMR spectra of poly(oxetane-*co*-tetrahydropyran) obtained in bulk at 35 °C; at different times using $BF_3{:}CH_3OH$ initiator (series S5 Table S3, Figures S5, S6, and S9) with $[Ox]_0$ = 1 M and $[BF_3{:}CH_3OH]_0$ = 7.7 mM; at different time with $C_2H_5OCH_2(THP)^+$,$[SbF_6]^-$ (EMOA) initiator (series S1−S4, S6, S7; Tables S1 and S2, Figures S1(ii), S2, S3(ii), S4, and S8) with $[EMOA]_0$ = 1.115 mM and various monomer feed composition f_{Ox} (0.1674, 0.1363, 0.04615, 0.0244) (series S1, S2, S6, S7, respectively), with f_{Ox} = 0.1363 M at various $[EMOA]_0$ (0.5, 1.115, 2.3 mM) (series S3, S2, S4, respectively); DSC thermogram of poly(oxetane-*co*-1,4-dioxane) (Figure S7.3) and poly(oxetane-*co*-tetrahydropyran) (Figures S7.1 and S7.2). This material is available free of charge via the Internet at http://pubs.acs.org.

References and Notes

(1) Inoue, S.; Aida, T. In *Ring-Opening Polymerization*; Ivin, K. J., Saegusa, T., Eds.; Elsevier Applied Science Publishers Ltd.: London, 1984; Vol. *1*, pp 185−298.
(2) Saegusa, T.; Matsumoto, S. *Macromolecules* **1968**, *1*, 442–5. Saegusa, T.; Matsumoto, S. *J. Macromol. Sci., Chem.* **1970**, *4*, 873–84.
(3) Saegusa, T. *J. Macromol. Sci., Chem.* **1972**, *6*, 997–1026.
(4) Saegusa, T.; Shiota, T.; Matsumoto, S.; Fujii, S. *Macromolecules* **1972**, *5*, 34–6.
(5) Saegusa, T.; Hashimoto, Y.; Matsumoto, S. *Macromolecules* **1971**, *4*, 1–3.
(6) Kobayashi, S.; Morikawa, K.; Saegusa, T. *Macromolecules* **1975**, *8*, 952–4.
(7) Pruckmayer, G.; Wu, T. K. *Macromolecules* **1973**, *6*, 33–8.
(8) Rosenberg, B. A. *Vysokomol. Soedin.* **1977**, *19B*, 510–516.
(9) Matyjaszewski, K.; Kubisa, P.; Penczek, S. *J. Polym. Sci.* **1974**, *12*, 1333–6.
(10) Matyjaszewski, K.; Penczek, S. *J. Polym. Sci.* **1974**, *12*, 1905–12.
(11) Pruckmayer, G.; Wu, T. K. *Macromolecules* **1975**, *8*, 954–6.
(12) Liu, Y. L.; Hsiue, G. H.; Chiu, Y. C. *J. Polym. Sci., Polym. Chem.* **1994**, *32*, 2543–9.
(13) Kobayashi, S.; Danda, H.; Saegusa, T. *Bull. Chem. Soc. Jpn.* **1974**, *47*, 2699–705.
(14) Kobayashi, S.; Danda, H.; Saegusa, T. *Macromolecules* **1974**, *7*, 415–20.
(15) Pruckmayer, G.; Wu, T. K. *Macromolecules* **1975**, *8*, 77–8.
(16) Kobayashi, S.; Tsuchida, N.; Morikawa, K.; Saegusa, T. *Macromolecules* **1975**, *8*, 386–90.
(17) Saegusa, T.; Kobayashi, S. *J. Polym. Sci., Polym. Symp.* **1976**, *56*, 241–53.
(18) Kobayashi, S.; Tsuchida, N.; Morikawa, K.; Saegusa, T. *Macromolecules* **1975**, *8*, 942–4.
(19) Dreyfuss, P.; Dreyfuss, M. P. *Adv. Polym. Sci.* **1967**, *4*, 528–90.

(20) Matyjaszewski, K.; Slomkoski, S.; Penczek, S. *J. Polym. Sci.* **1979**, *17*, 2413–22.
(21) Brzezinska, K.; Matyjaszewski; Penczek, S. *Makromol. Chem.* **1978**, *179*, 2387–95.
(22) (a) Bernaerts, K. V.; Schacht, H. S.; Goethals; Du Prez, F. E. *J. Polym. Sci., Part A: Polym. Chem.* **2003**, *41*, 3206–17. (b) Tasdelen, M., A.; Van Camp, M.; Goethals, E.; Dubois, P.; Du Prez, F.; Yagaci, Y. *Macromolecules* **2008**, *41*, 6035–40.
(23) Worsfold, D. J.; Eastham, A. M. *J. Am. Chem. Soc.* **1957**, *79*, 900–2.
(24) Latremouille, G. A.; Merrall, G. T.; Eastham, A. M. *J. Am. Chem. Soc.* **1960**, *82*, 120–4.
(25) Kuntz, I. *J. Polym. Sci., Part A-1* **1967**, *5*, 193–203.
(26) Dale, J. *CHEMTECH* **1975**, 3.
(27) Dale, J.; Daasvatn, K.; Groenneberg, T. *Makromol. Chem.* **1977**, *178*, 873–9.
(28) Kobayahsi, S.; Morikawa, K.; Saegussa, T. *Polym. J.* **1979**, *11*, 405–12.
(29) Rose, J. B. *J. Chem. Soc.* **1956**, 542–6.
(30) Rose, J. B. *J. Chem. Soc.* **1956**, 546–55.
(31) Farthing, A. C.; Reynolds, R. J. *J. Polym. Sci.* **1954**, *12*, 503–7.
(32) Natta, G.; Dall'Asta, G.; Porri, L. *Makromol. Chem.* **1965**, *81*, 253–7.
(33) Dreyfuss, P.; Dreyfuss, M. P. *Polym. J.* **1976**, *8*, 81–7.
(34) Bucquoye, M. R.; Goethals, E. J. *Makromol. Chem.* **1978**, *179*, 1681–8.
(35) Sasaki, H.; Rudzinski, J. M.; Kakuchi, T. *J. Polym. Sci., Part A: Polym. Chem.* **1995**, *33*, 1807–16.
(36) Bucquoye, M. R.; Goethals, E. J. *Polym. Bull.* **1980**, *2*, 707–712.
(37) *Makromol. Chem.* **1981**, *182*, 3379−86.
(38) (a) Bouchékif, H.; Philbin, M. I.; Colclough, E.; Amass, A. J. IUPAC international symposium on ionic polymerization, Hersonisos, Crete, **2001**, B09. (b) Bouchékif, H.; Philbin, M. I.; Colclough, E.; Amass, A. J. *Chem. Commun.* **2005**, *30*, 3870–2. (c) Bouchékif, H.; Philbin, M. I.; Colclough, E.; Amass, A. J. *Chem. Commun.* **2005**, *30*, 3873–4.
(39) Bouchékif, H.; Philbin, M. I.; Colclough, E.; Amass, A. J. *Macromolecules* **2008**, *41*, 1989–95.
(40) Matyjaszewski, K.; Zielinski, M.; Kubisa, P.; Slomkowski, S.; Chojnowski, J.; Penczek, S. *Makromol. Chem.* **1980**, *181*, 1469–82.
(41) Slomkowski, S. *Makromol. Chem.* **1985**, *186*, 2581–94.
(42) Searles, S.; Tamres, M.; Lippincott, E. R. *J. Am. Chem. Soc.* **1953**, *75*, 2775–6.
(43) Arnett, A. M. *Prog. Phys. Org. Chem.* **1967**, *7*, 243.
(44) Yamashita, Y.; Tsuda, T.; Okada, M.; Iwatsuki, S. *J. Polym. Sci., Part A: Polym. Chem.* **1966**, *4*, 2121–35.
(45) Slomkowski, S.; Penczek, S. *J. Chem. Soc., Perkin Trans. 2* **1974**, *14*, 1718–22.
(46) Aoshima, A.; Fujisawa, T.; Kobayashi, E. *J. Polym. Sci., Part A: Polym. Chem.* **1994**, *32*, 1719–28.
(47) Burgess, F. J.; Cunliffe, A. V.; MacCallum, J. R.; Richards, D. H. *Polymer* **1977**, *18*, 726–732.
(48) Dubreuil, M. F.; Farcy, N. G.; Goethals, E. J. *Makromol. Rapid Commun.* **1999**, *20*, 383–6.
(49) Furukawa, J. *Polymer* **1962**, *3*, 487–509.
(50) Matyjaszewski, K.; Slomkowski, S.; Penczek, S. *J. Polym. Sci.* **1979**, *17*, 69–80.
(51) Shieh, Y. T.; Lay, M. L.; Chen, S. A. *J. Polym. Res.* **2003**, *10*, 151–60.
(52) Sharavanan, K.; Ortega, E.; Moreau, M.; Lorthioir, C.; Lauprêtre, F.; Desbois, P.; Klatt, M.; Vairon, J. P. *Macromolecules* **2009**, *42*, 8707–10.
(53) Moad, G.; Moad, C. L.; Rizzardo, E.; Thang, S. H. *Macromolecules* **1996**, *29*, 7717–26.
(54) Chong, Y. K.; Le, G, T. P. T.; Rizzardo, E.; Thang, S. H. *Macromolecules* **1999**, *32*, 2071–74.
(55) *Handbook of Radical Polymerization*; Matyjaszewski, K., Davis, T. P., Eds.; Wiley Publishers: Hoboken, 2002; pp 444−8.
(56) Perrier, S.; Barner-Kowollik, C.; Quinn, J. F.; Vana, P.; Davis, T. P. *Macromolecules* **2002**, *35*, 8300–06.
(57) Barner-Kowollik, C.; Coote, M. L.; Davis, T. P.; Radom, L.; Vana, P. *J. Polym. Sci., Part A: Polym. Chem.* **2003**, *41*, 2828–32.
(58) Wang, A. R.; Zhu, S.; Kwak, Y.; Goto, A.; Fukuda, T.; Monteiro, M. S. *J. Polym. Sci., Part A: Polym. Chem.* **2003**, *41*, 2833–9.
(59) Rizzardo, E.; Chiefari, J.; Mayadunne, R. T. A.; Moad, G.; Thang, S. H. *ACS Symp. Ser.* **2000**, *768*, 278–96.
(60) Chong, Y. K.; Krstina, J.; Le, T. P. T.; Moad, G.; Postma, A.; Rizzardo, E.; Thang, S. H. *Macromolecules* **2003**, *36*, 2256–2272.
(61) Moad, G.; Mayadunne, R. T. A.; Rizzardo, E.; Skidmore, M.; Thang, S. H. *ACS Symp. Ser.* **2003**, *854*, 520–35.
(62) Delaittre, G.; Charleux, B. *Macromolecules* **2008**, *41*, 2361–67.
(63) Saegusa, T.; Fujii, H.; Kobayashi, S.; Ando, H.; Kawase, R. *Macromolecules* **1973**, *6*, 26–32.